Two-dimensional and three-dimensional Coulomb clusters in parabolic traps

L. G. D'yachkov, M. I. Myasnikov, O. F. Petrov, T. W. Hyde, J. Kong, and L. Matthews

Citation: Physics of Plasmas (1994-present) **21**, 093702 (2014); doi: 10.1063/1.4885637
View online: http://dx.doi.org/10.1063/1.4885637
View Table of Contents: http://scitation.aip.org/content/aip/journal/pop/21/9?ver=pdfcov
Published by the AIP Publishing

Two-dimensional and three-dimensional Coulomb clusters in parabolic traps

L. G. D'yachkov,[1,a)] M. I. Myasnikov,[1,b)] O. F. Petrov,[1,2,3] T. W. Hyde,[3] J. Kong,[3] and L. Matthews[3]
[1]*Joint Institute for High Temperatures, Russian Academy of Sciences, Moscow 125412, Russia*
[2]*Moscow Institute of Physics and Technology (State University), Dolgoprudny 141700, Moscow Region, Russia*
[3]*Center for Astrophysics, Space Physics, and Engineering Research (CASPER), Baylor University, Waco, Texas 76798-7310, USA*

(Received 18 April 2014; accepted 14 June 2014; published online 8 September 2014)

We consider the shell structure of Coulomb clusters in an axially symmetric parabolic trap exhibiting a confining potential $U_c(\rho, z) = (m\omega^2/2)(\rho^2 + \alpha z^2)$. Assuming an anisotropic parameter $\alpha = 4$ (corresponding to experiments employing a cusp magnetic trap under microgravity conditions), we have calculated cluster configurations for particle numbers $N = 3$ to 30. We have shown that clusters with $N \leq 12$ initially remain flat, transitioning to three-dimensional configurations as N increases. For $N = 8$, we have calculated the configurations of minimal potential energy for all values of α and found the points of configuration transitions. For $N = 13$ and 23, we discuss the influence of both the shielding and anisotropic parameter on potential energy, cluster size, and shell structure. © *2014 AIP Publishing LLC*. [http://dx.doi.org/10.1063/1.4885637]

I. INTRODUCTION

Dusty plasma is of interest both for future technological applications and as an object of basic research.[1,2] In recent years, increased attention has been given to the investigation of dust clusters containing several to thousands of particles as possible analogues for strongly coupled Coulomb systems and non-neutral plasmas.[3–6] It has already been shown that restructuring of such clusters can provide details concerning phase transitions in other systems. Two-dimensional (2D) clusters formed in the sheath of a rf discharge[7–11] and three-dimensional (3D) clusters, particularly those exhibiting spherical symmetry, have also been examined[5,7–13] both theoretically and experimentally. Most frequently, clusters of this sort are formed in axially symmetric parabolic traps, where the particles are confined by the potential

$$U_c(\rho, z) = \frac{1}{2} m\omega^2(\rho^2 + \alpha z^2), \tag{1}$$

where m is the mass of the particle, ω is the frequency of harmonic oscillations in the $x-y$ plane ($\rho^2 = x^2 + y^2$) about the equilibrium point $\rho = 0$, the frequency of oscillations in a perpendicular direction (along axis z) is $\omega\alpha^{1/2}$, and α is the anisotropic parameter. For the case of spherical symmetry $\alpha = 1$, while the 2D case corresponds to $\alpha \gg 1$. The resulting shell structures formed in both cases have been studied in detail for both Coulomb[5,11,13–15] and Yukawa clusters[8,16,17] and the conditions for the formation of mono- and few-layered structures identified.[18–20] Coulomb cluster configurations in anisotropic traps at various values of $\alpha < 1$ have been investigated[15,21] and the formation of chain and helical structures[22–25] ($\alpha \ll 1$) have been identified. Specifically, the gradual transition from a flat configuration (square) to a vertical chain as α decreases was examined for clusters with $N = 4$.[21] The restructuring of laterally compressed flat Coulomb and Yukawa clusters has also been investigated.[10,26]

Recently, we proposed a magnetic trap[27–29] for Coulomb clusters consisting of diamagnetic dust particles in a non-ionized medium as a possible alternative to the electrostatic traps employed in gas discharge plasmas.[1,30] A similar method was used previously for the levitation of single uncharged macroscopic bodies.[31,32] In a nonuniform steady-state magnetic field, particles are acted upon by an effective force $\mathbf{F}_B(\mathbf{r}) = -(m\chi/2)\nabla\mathbf{B}^2(\mathbf{r})$,[31,33] where χ is the specific magnetic susceptibility dependent upon the composition of the particle. For diamagnets, $\chi < 0$, so diamagnetic particles will be located in a magnetic well. In our first experiments under terrestrial conditions,[27–29] electromagnet pole tips of a special form have been designed for the creation of a magnetic trap; graphite particles were charged upon contact with a conducting probe made in the form of pointed needle and formed a cluster. However, in the terrestrial laboratory setup, we have obtained only small clusters containing a few particles. Then in a cusp magnetic trap operating under microgravity conditions, we have observed Coulomb clusters with structures similar to an oblate ellipsoid of revolution and containing thousands of graphite particles.[34,35] In this trap, the magnetic field is axially symmetric and can be approximated by linear dependences on the coordinates, so $\mathbf{B}^2(\rho, z) = A^2(\rho^2 + \alpha z^2)$, where A depends on the current in the electromagnet coils and $\alpha = 4$. Thus, we have a parabolic trap with $\omega^2 = |\chi|A^2$. In the trap, the particles were charged by contacting with a central wire electrode of diameter 200 μm that passed along the z axis of the trap. The thickness to diameter ratio for the clusters was experimentally shown to be close to the theoretical value for that found for a uniformly charged fluid, i.e., 0.2934 for $\alpha = 4$. However, small clusters containing only a few particles in such a trap should be flat.

[a)]E-mail: dyachk@mail.ru.
[b)]E-mail: miasnikovmi@mail.ru.

In this paper, we consider the shell structure exhibited by small clusters under the conditions described for a cusp magnetic trap ($\alpha = 4$) and the transition of two-dimensional (2D) clusters to three-dimensional (3D) ones as the number of particles, N, in the cluster increases. For certain values of N, we have also considered the dependence of the cluster's structure and potential energy on the anisotropic parameter and shielding.

II. COULOMB CLUSTERS WITH $N = 3$ TO 30

We begin by employing a MD simulation to calculate the structural formation of Coulomb clusters containing 3 to 30 particles from an initially random distribution having zero velocity and confined in a parabolic trap at $\alpha = 4$. We assume that all the particles are spherical, have the same radius a and mass m_p and carry identical charges q_p. Their movement is then described by the system of Newtonian equations ($1 < k < N$):

$$m_p \frac{d^2\mathbf{r}_k}{dt^2} = \sum_{l \neq k} \frac{q_p^2 \mathbf{r}_{kl}}{|\mathbf{r}_{kl}|^3} - \nabla U_c(\mathbf{r}_k) - 6\pi\eta a \mathbf{u}_k, \qquad (2)$$

where $\mathbf{r}_k$ is the position of the center of a particle k, $\mathbf{r}_{kl} = \mathbf{r}_k - \mathbf{r}_l$, $\mathbf{u}_k$ is the particle's velocity relative to the medium, and η is the viscosity of the medium. In the simulation, we assumed an argon medium held at atmospheric pressure as in the experiment described in Refs. 34 and 35. The first term in the right-hand side of Eq. (2) represents the electrostatic interaction between particles, the second term is the confining force as determined by Eq. (1), and the third term is the force of friction against the medium. Here we consider cluster configurations at zero temperature; since the last term is a dissipative force needed only for temperature reduction, its value affects only cluster formation time, so the values of η and a may be ignored. Clusters with $N = 3$ to 13 were calculated by minimization of the potential energy. In the simplest case, for a ground configuration with $N \leq 8$, the solution can be obtained analytically. Both methods lead to the same results with high accuracy.

All calculations were performed employing length and energy units

$$l_0 = (2q_p^2/m_p\omega^2)^{1/3}, \; E_0 = q_p^{4/3}(m_p\omega^2/2)^{1/3}, \qquad (3)$$

with the results also presented in this manner. A physical significance of the quantities in Eq. (3) is following: $U_c = E_0$ at $(\rho, z) = (l_0, 0)$, and E_0 is the Coulomb interaction energy of two particles at a distance l_0.

All clusters having $N \leq 12$ (for $\alpha = 4$) were found to be flat, with 2D to 3D transitions beginning at $N = 13$ and occurring initially in the inner shell. For the case of 2D clusters ($N \leq 12$), both the shell structure and calculated energies were found to coincide exactly with those obtained using a Monte Carlo method.[14] As can be seen below, for $N \geq 13$, the energy of the ground state for 3D structures is obviously lower than that of the ground state for flat ones.

Configurations of representative 2D clusters obtained in the manner described are presented in Fig. 1. The top and side views of clusters having $N = 13$, 16, and 17 are shown in Fig. 2.

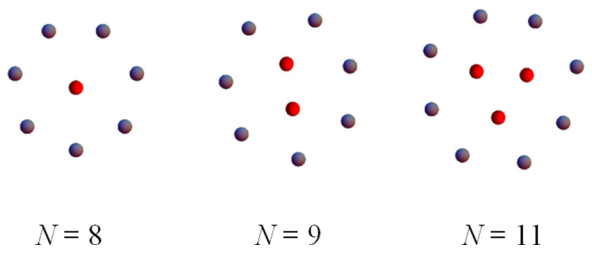

FIG. 1. Shell structure for representative clusters consisting of $N = 8$, 9, and 11 particles and confined in a parabolic trap at $\alpha = 4$.

For $N \leq 5$ all particles are located at the corners of a regular polygon with the sixth particle localized at the center of the cluster. A second particle appears within the central shell at $N = 9$, a third at $N = 11$, a fourth at $N = 13$ (see Fig. 2), and a fifth at $N = 15$. At $N = 16$, a third shell arises in the center, with the shell structure now presented as (1, 5, 10).[14] This sequence corresponds to the filling of shells in the flat clusters; however, the similarity between shell structures ends at the top view. For example in the case of $N = 13$, the inner shell is split with two particles located above the outer shell plane and two below; we write this shell structure as (2 + 2, 9). The top view begins to differ from that for flat clusters at $N = 17$. In the 2D cluster the shell structure is (1, 6, 10),[14] while in the 3D case it is (3 + 3, 11) and exhibits no central particle. The internal 6 particles are located at the vertices of two regular triangles, shifted in opposite directions relative to the outer shell plane and rotated relative to one another by 60°.

In Fig. 3, we present the structure of clusters consisting of $N = 23$ and 26, and in Fig. 4 the structure of clusters with $N = 29$ and 30. Shell structure is clearly visible in the top view; however, the degree of symmetry is less pronounced than that seen in flat clusters, especially for the inner shells, which are split. (This can be clearly seen from the side.) A top view of the shell structure developed within a 3D cluster with $N = 23$ is close in appearance to that seen in the 2D version (2, 8, 13), but the structure of clusters with $N = 26$, 29, and 30 is significantly different from their corresponding flat versions, (3, 9, 14), (5, 10, 14) and (5, 10, 15), respectively.[14] It can also be seen that the shape of the cluster gradually approaches that of an oblate ellipsoid of revolution, although the outer shell remains almost flat throughout. The cluster

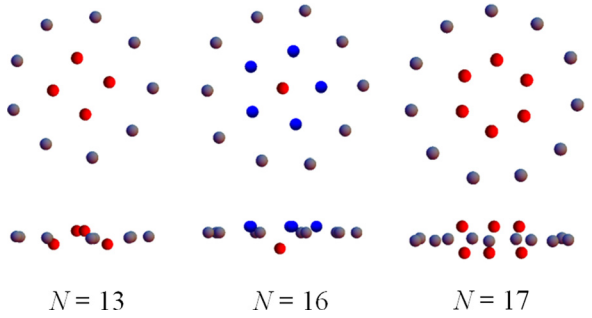

FIG. 2. Representative clusters having $N = 13$, 16, and 17 particles and confined in a parabolic trap at $\alpha = 4$. Both top and side views.

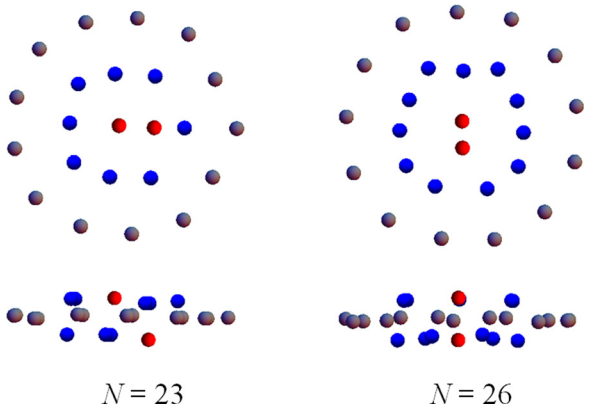

FIG. 3. Representative clusters with $N = 23$ and 26 particles and confined in a parabolic trap at $\alpha = 4$. Both top and side views.

thickness to diameter ratio H_c/D_c and the number of particles in a cluster confined in a parabolic trap at $\alpha = 4$ are presented in Fig. 5.

III. DEPENDENCE OF POTENTIAL ENERGY ON α FOR A CLUSTER WITH $N = 8$

It is also interesting to consider the dependence of the cluster's structural symmetry on the anisotropic parameter α. At $\alpha \gg 1$, the cluster configuration is in general two-dimensional (2D), becoming three-dimensional (3D) as α decreases and then collapsing into a linear chain for the case $\alpha \ll 1$. For smaller clusters ($N = 4$), the relationship between cluster configuration and the anisotropic parameter α was recently considered in detail by Kamimura *et al.*[21] We expand here on their results by considering the dependence of the cluster's potential energy on α for select values of N and noting the subsequent change in cluster structure.

The dependence on α of a cluster's ($N = 8$) potential energy across various configurations can be seen in Fig. 6. While the cluster can exist in any of several different structural states for a given value of α, the configuration with the lowest energy represents the ground-state condition. Where two different states have the same energy, the configurations are metastable and a transition between states will occur as α increases or decreases.

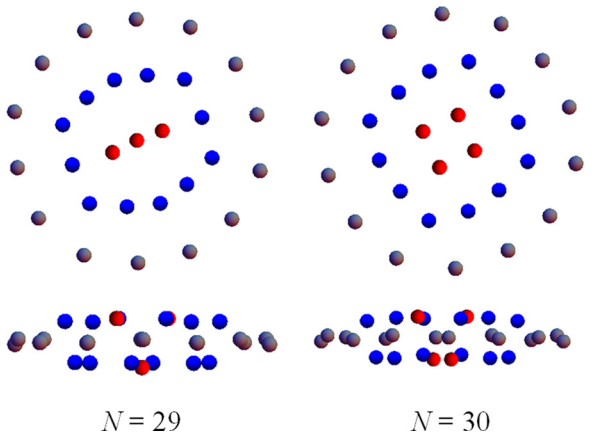

FIG. 4. Representative clusters with $N = 29$ and 30 particles and confined in a parabolic trap at $\alpha = 4$. Both top and side views.

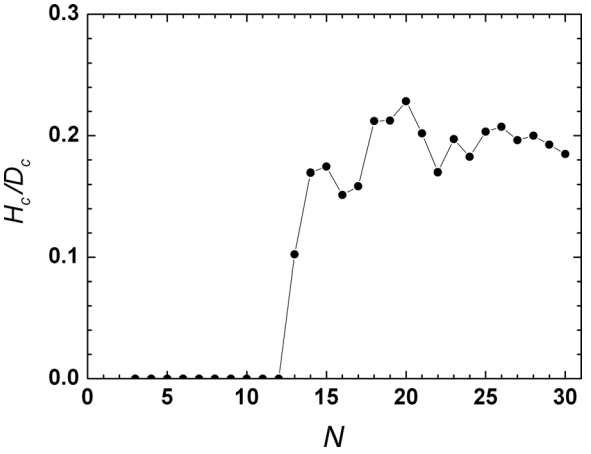

FIG. 5. Dependence of the ratio of cluster thickness H_c and diameter D_c on the number of particles N for a cluster confined in a parabolic trap at $\alpha = 4$.

For a cluster ($N = 8$) in the ground configuration (i.e., configuration of minimum energy) and $\alpha > 2.73$, the cluster exhibits a structural symmetry of a flat regular heptagon with a central particle (see Fig. 1); in this case, the energy $U/E_0 = 29.3512$ is not obviously dependent on α (see the red horizontal line *a* in Fig. 6). For $\alpha < 2.73$, this configuration becomes metastable with the ground state appearing as a regular hexagon with one central particle on the top and another central particle on the bottom. This is shown in Fig. 7(a), while its energy (as shown by the violet dashed curve *b*) can

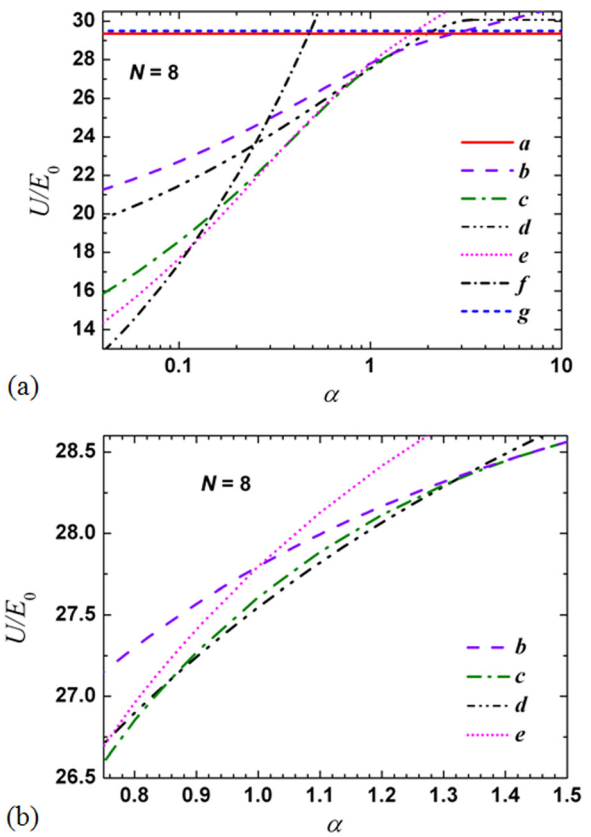

FIG. 6. Dependence of the cluster's potential energy ($N = 8$) on the anisotropic parameter α. (a) Cluster restructuring beginning with a linear chain ($\alpha \ll 1$) and transitioning to a flat configuration ($\alpha \gg 1$); (b) area of intersection of several curves on a larger scale.

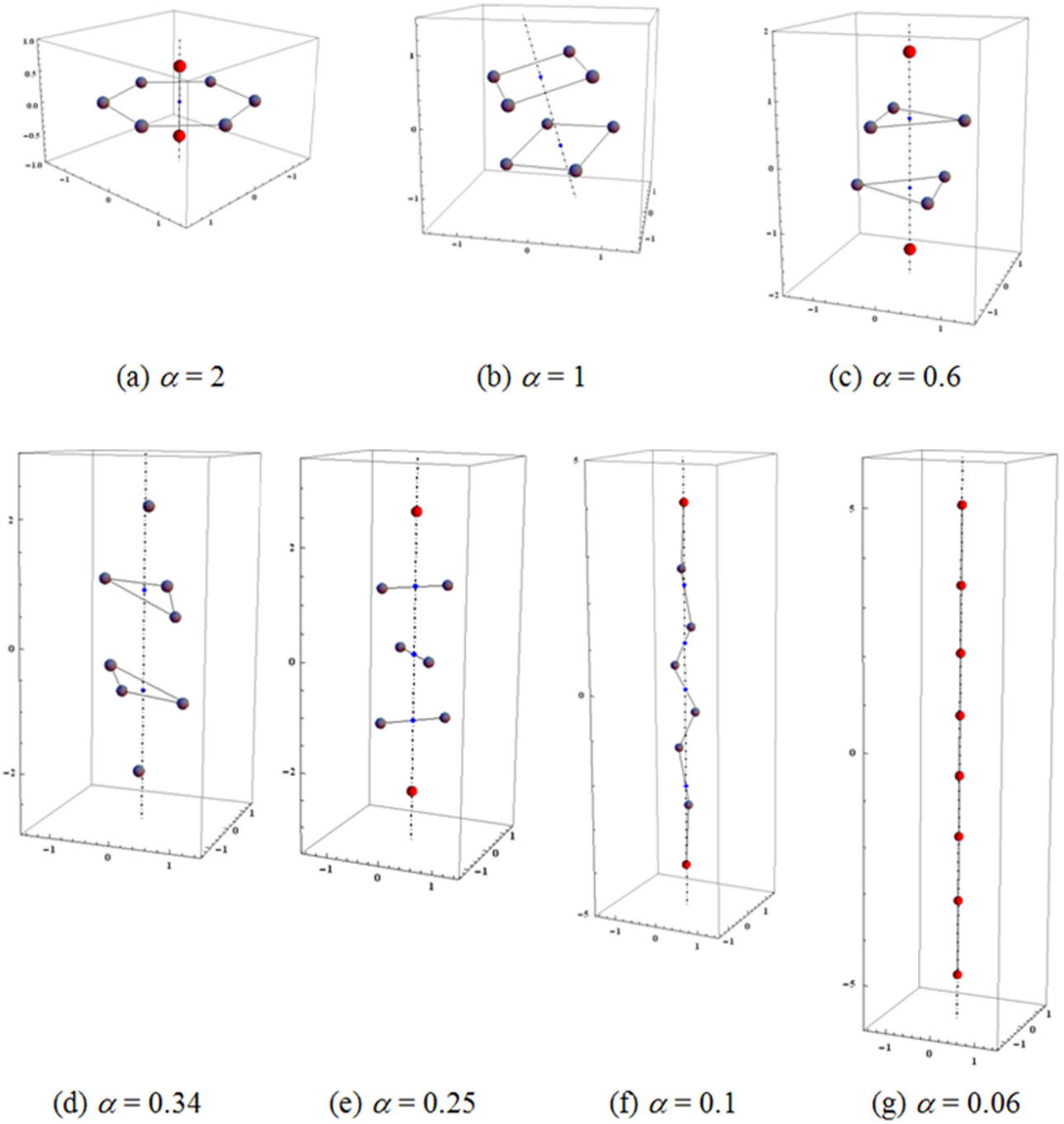

FIG. 7. Ground configurations for a cluster with $N = 8$ at various values of α: (a) $\alpha = 2$ where the configuration shown corresponds to the dashed violet curve *b* in Fig. 6; (b) $\alpha = 1$ where the configuration shown corresponds to the dashed-double-dotted black curve *d*; (c) $\alpha = 0.6$ where the configuration shown corresponds to the dashed-dotted green curve *c*; (d) $\alpha = 0.34$, (e) $\alpha = 0.25$ where the configurations shown corresponds to the dotted magenta curve *e*; (f) $\alpha = 0.1$; (g) $\alpha = 0.06$ where the configuration shown corresponds to the short dashed-dotted black curve *f*. The particles on axis are shown in red. (Note that the top and bottom particles in (d) are displaced from the axis.)

be seen in Fig. 6. At $\alpha \approx 1.4$, the hexagon splits into two equilateral triangles in parallel planes (see the green dashed-dotted curve *c* in Fig. 6 and configuration in Fig. 7(c)). It is interesting to note that configurations having approximately the same energies are also possible. For example, the configuration shown in Fig. 7(c) is in the ground state for $1.32 < \alpha < 1.4$ and $\alpha < 0.86$, while for $0.86 < \alpha < 1.32$, it is in a metastable state.

Within the interval, $0.86 < \alpha < 1.32$, the ground state configuration consists of two sets of four particles in parallel planes. In each plane, these particles are located at the corners of two squares rotated by an angle of $\pi/4$ relative to each other; in other words, in a top view, it would be seen as a regular octagon. Its energy is represented by a black dashed-double dotted curve *d* in Fig. 6. The isotropic case ($\alpha = 1$) is shown in Fig. 7(b), for an arbitrary axis of symmetry. For $\alpha = 1$, the potential energy of the ground configuration $U/E_0 = 27.5473$ is 0.22% less than that of the cubic configuration incorrectly reported as the ground state in Ref. 36. Outside the interval $0.86 < \alpha < 1.32$, this configuration

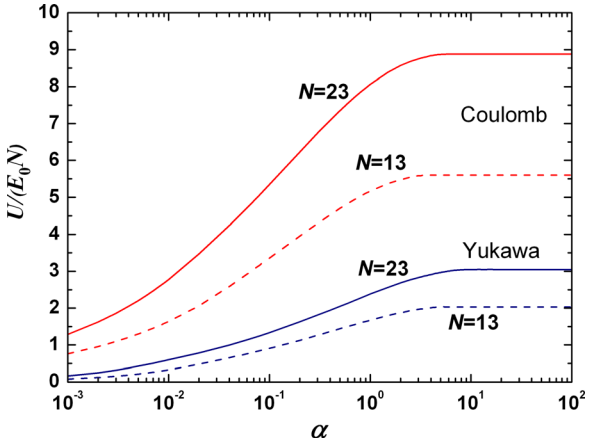

FIG. 8. Potential energy for $N=13$ (dashed curves) and $N=23$ (solid curves) Coulomb (red) and Yukawa (blue) clusters as a function of the anisotropic parameter.

becomes metastable; at $\alpha > 3.41$ the planes of the squares coincide and the configuration becomes a flat octagon (see the horizontal part of the curve). For $\alpha < 0.86$, the ground configuration becomes again two equilateral triangles in parallel planes, rotated by an angle of $\pi/3$ relative to each other, with two single particles on the top and bottom (see the green dashed-dotted curve *c* in Fig. 6). The corresponding results for $\alpha = 0.6$ are shown in Fig. 7(c) where it can be seen that the distance between planes increases as α decreases. At $\alpha \approx 0.34$, the triangles are deformed (see Fig. 7(d)) and devolve into three pairs of particles, located one above another and rotated by 90 degrees with respect to those located underneath (see Fig. 7(e) and the magenta dotted curve *e* in Fig. 6). At $\alpha \approx 0.12$, the particles are drawn into the familiar zigzag chain lying in a vertical plane (Fig. 7(f)), becoming linear at $\alpha = 0.06$ (see Fig. 7(g) and the short black dashed-dotted curve *f* in Fig. 6(a)) In addition to these

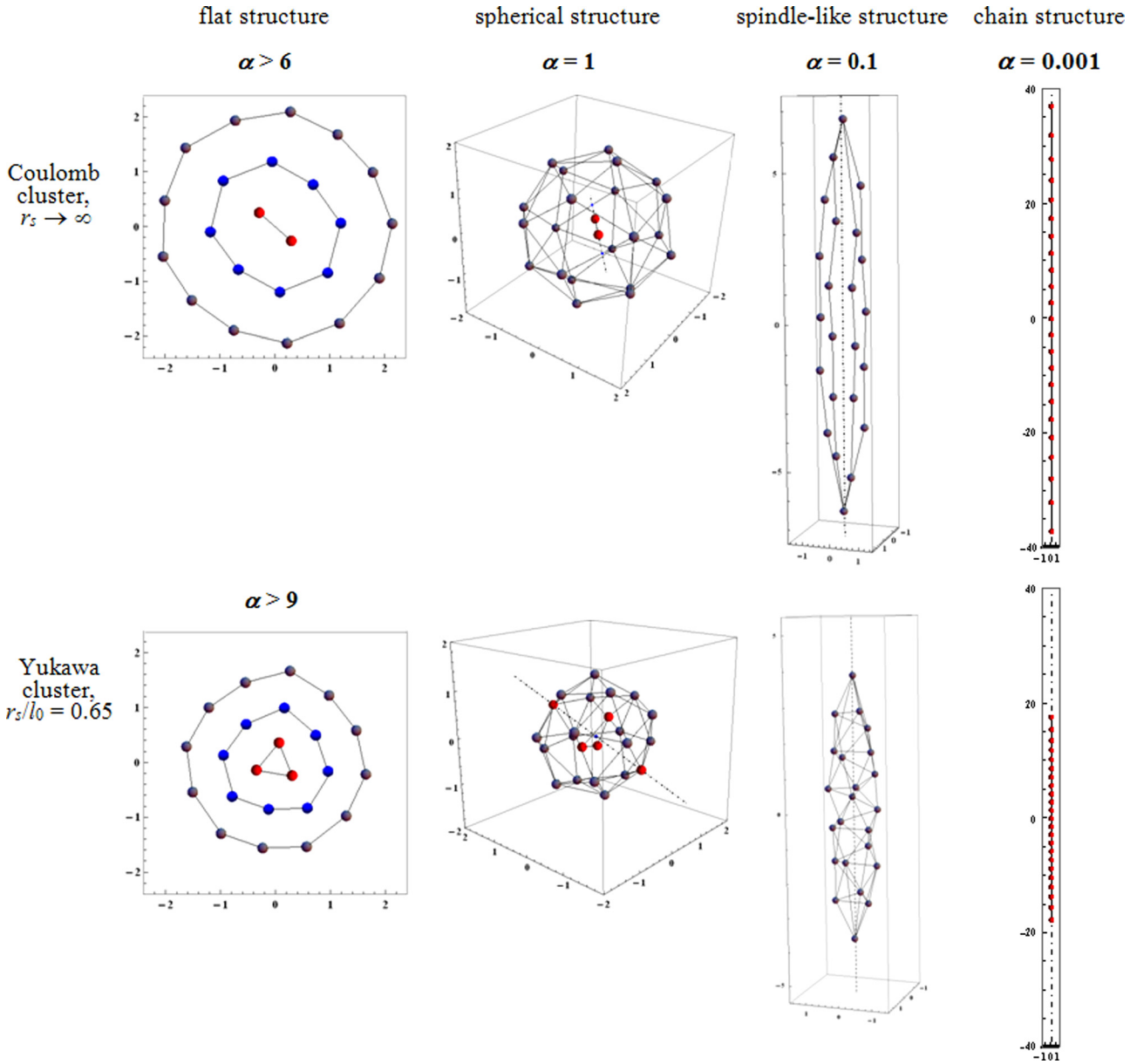

FIG. 9. Representative shell structures for Coulomb and Yukawa ($N=23$ and $r_s/l_0=0.65$) clusters for four values of the anisotropic parameter: $\alpha > 6$ for Coulomb and $\alpha > 9$ for Yukawa (flat configuration), $\alpha = 1$ (isotropic configuration), $\alpha = 0.1$ (spindle-like configuration) and $\alpha = 0.001$ (chain configuration). The particles in the inner shell and on the axis are shown in red where it should be noted that for $\alpha = 0.1$ no particle is exactly on the axis.

ground configurations, we show in Fig. 6(a) the energy of the flat configuration (2, 6) with two particles in the inner shell, $U/E_0 = 29.4990$ (see short blue dashed horizontal line g) which is metastable for all values of α. Such a configuration has also been observed in the sheath of rf discharge,[7] where the dust structure was planar and multilayer, besides the dust particle charges were apparently partly shielded. It should be noted that the metastable configurations discussed may have higher probabilities of occurring than do their corresponding ground states[17] and may be the only ones actually appearing in both experiments and numerical simulations.

IV. EFFECT OF SHIELDING

As expected, the number of possible cluster configurations rapidly increases with N. For $N = 13$ and 23, Fig. 8 shows the potential energy as a function of the anisotropic parameter for ground states. These clusters will remain flat at $\alpha > 4.3$ and $\alpha > 6$, respectively. Most experiments with dust clusters were performed in electrodischarge plasma where screening of the dust particle charges occurs. Therefore, it is interesting the difference in the cluster structures in nonionized medium of our magnetic trap[34,35] and in electrostatic traps in discharge plasmas. So, we also show in Fig. 8 the effect of shielding (see blue curves) for $r_s/l_0 = 0.65$, where r_s is the shielding length and l_0 is determined by Eq. (3). (This value of the ratio r_s/l_0 corresponds to the experimental conditions observed in Ref. 7.) Increased shielding leads to a weakening of the interparticle repulsion and consequently to a decrease in both cluster size and potential energy. Besides the points of the transition to flat configuration are shifted to $\alpha = 5.8$ for $N = 13$ and $\alpha = 9$ for $N = 23$.

In Fig. 9, we present ground state configurations for both Coulomb and Yukawa clusters, with $N = 23$, across four cases: 2D structures ($\alpha > 6$ for Coulomb and $\alpha > 9$ for Yukawa), spherically symmetric structures ($\alpha = 1$), spindle-like structures ($\alpha = 0.1$) and chain structures ($\alpha = 0.001$). For $\alpha = 4$, the 3D structure of the Coulomb cluster can be seen in Fig. 3. While the primary effect of the shielding is simply a reduction in cluster size and potential energy,[37] it can be seen

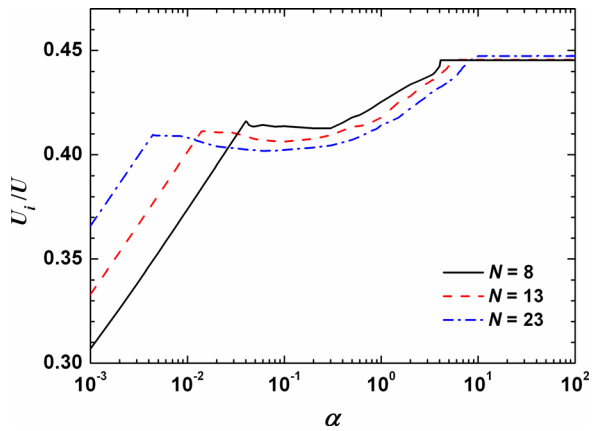

FIG. 10. The ratio of the energy of interaction between particles U_i and the total potential energy U for Yukawa clusters ($N = 8$, 13, and 23) as a function of the anisotropic parameter.

that enhanced shielding can also lead to transformation of the shell structure. In the 2D shell structure of the flat Coulomb cluster (2, 8, 13), one particle passes from the outer shell to the inner shell when shielding is included, while for the Yukawa cluster (at $r_s/l_0 = 0.65$) we see an entirely new configuration (3, 8, 12). For the isotropic ($\alpha = 1$) Yukawa cluster, two configurations (with two and three particles in the inner shell) exhibit almost identical energies and both appear in the MD simulations. However, for the configuration having three particles in the inner shell, the energy is lower by $0.0053E_0$.

A relation between the strength of the trap and the strength of the electrostatic interaction between particles is interesting too. For all Coulomb clusters, the interaction energy between particle U_i is twice the energy of interaction with the trap U_c at any α. For Yukawa clusters, the particle interaction is weakened and corresponding energy U_i is less than half of the total energy $U = U_c + U_i$. In Fig. 10, we present the dependence of the ratio U_i/U on α for Yukawa clusters with $N = 8$, 13, and 23. All the curves consist of three parts. The right horizontal part corresponds to 2D configurations, the straight part on the left corresponds to 1D chains, and the middle part corresponds to 3D configurations. Increasing the number of particles N leads to expansion of the middle 3D part.

V. CONCLUSIONS

To summarize, we have considered small Coulomb clusters confined within axially symmetric parabolic traps, examining their transformation between two- and three-dimensional symmetries as the number of particles N in the cluster increases or the anisotropic parameter α decreases. For $\alpha = \text{const} > 1$, clusters with only a few particles retain a two-dimensional configuration, becoming three-dimensional as the number of particles increases. (As a single representative example, for $\alpha = 4$ this transition begins at $N = 13$.) For sufficiently large N, cluster configuration was shown to approach that of a uniformly charged fluid (i.e., an oblate ellipsoid of revolution).[35]

Additionally, the transformation from two- through three- to one-dimension as α decreases was also examined for clusters with $N = 8$. For this case, it was shown the cluster passes through many different configurations with its potential energy decreasing as α decreases. It was also found that for specific (critical) values of α, competing configurations with minimal energy differences are possible.

The effect of shielding on clusters with $N = 13$ and $N = 23$ has also been considered. As expected, increased shielding was shown to lead to a weakening of interparticle repulsion and consequently to a decrease in both cluster size and potential energy. In two- ($\alpha > 6$) and three-dimensional ($\alpha = 1$) cases, for the cluster with $N = 23$, enhanced shielding was also shown to lead to transformation of the shell structure itself, producing a Coulomb cluster containing two particles in the inner shell and a Yukawa cluster containing three particles located at the center of the configuration.

Finally, we have considered the relation between the contributions of the particle interaction and interaction with the trap into the cluster potential energy.

ACKNOWLEDGMENTS

This study was supported in part by the Program "Thermophysics and Mechanics of Extreme Energy Actions" of the Presidium of the Russian Academy of Sciences and by the RFBR Project Nos. 14-02-31226, 13-02-01393, and 13-02-12256.

[1]V. E. Fortov and G. E. Morfill, *Complex and Dusty Plasmas* (CRC Press, London, 2010).
[2]P. K. Shukla and B. Eliasson, Rev. Mod. Phys. **81**, 25 (2009).
[3]M. Bonitz, C. Henning, and D. Block, Rep. Prog. Phys. **73**, 066501 (2010).
[4]H. Baumgartner, D. Block, and M. Bonitz, Contrib. Plasma Phys. **49**, 281 (2009).
[5]O. Arp, D. Block, A. Piel, and A. Melzer, Phys. Rev. Lett. **93**, 165004 (2004).
[6]D. H. E. Dubin and T. M. O'Neil, Rev. Mod. Phys. **71**, 87 (1999).
[7]W. T. Juan, Z. Huang, J. Hsu, Y. Lai, and L. I, Phys. Rev. E **58**, R6947 (1998).
[8]H. Totsuji, C. Totsuji, and K. Tsuruta, Phys. Rev. E **64**, 066402 (2001).
[9]A. Melzer, Phys. Rev. E **67**, 016411 (2003).
[10]T. E. Sheridan and K. D. Wells, Phys. Rev. E **81**, 016404 (2010).
[11]V. A. Schweigert and F. M. Peeters, Phys. Rev. B **51**, 7700 (1995).
[12]P. Ludwig, S. Kosse, and M. Bonitz, Phys. Rev. E **71**, 046403 (2005).
[13]S. W. S. Apolinario, B. Partoens, and F. M. Peeters, New J. Phys. **9**, 283 (2007).
[14]V. M. Bedanov and F. M. Peeters, Phys. Rev. B **49**, 2267 (1994).
[15]S. W. S. Apolinario and F. M. Peeters, Phys. Rev. B **78**, 024202 (2008).
[16]M. Bonitz, D. Block, O. Arp, V. Golubnychiy, H. Baumgartner, P. Ludwig, A. Piel, and A. Filinov, Phys. Rev. Lett. **96**, 075001 (2006).
[17]H. Kählert, P. Ludwig, H. Baumgartner, M. Bonitz, D. Block, S. Käding, A. Melzer, and A. Piel, Phys. Rev. E **78**, 036408 (2008).
[18]O. S. Vaulina, K. G. Adamovich, and I. E. Dranzhevski, Plasma Phys. Rep. **31**, 562 (2005).
[19]O. S. Vaulina, X. G. Koss (Adamovich), and S. V. Vladimirov, Phys. Scr. **79**, 035501 (2009).
[20]I. I. Lisina and O. S. Vaulina, EPL **103**, 55002 (2013).
[21]T. Kamimura and Y. Suga, Phys. Plasmas **14**, 123706 (2007).
[22]O. S. Vaulina, I. I. Lisina, and X. G. Koss, Plasma Phys. Rep. **39**, 394 (2013).
[23]T. Kamimura and O. Ishihara, Phys. Rev. E **85**, 016406 (2012).
[24]J. Kong, T. W. Hyde, L. Matthews, K. Qiao, Z. Zhang, and A. Douglass, Phys. Rev. E **84**, 016411 (2011).
[25]T. W. Hyde, J. Kong, and L. S. Matthews, Phys. Rev. E **87**, 053106 (2013).
[26]O. Rancova, E. Anisimovas, and T. Varanavičius, Phys. Rev. E **83**, 036409 (2011).
[27]S. F. Savin, L. G. D'yachkov, M. M. Vasiliev, O. F. Petrov, and V. E. Fortov, Europhys. Lett. **88**, 64002 (2009).
[28]S. F. Savin, L. G. D'yachkov, M. M. Vasiliev, O. F. Petrov, and V. E. Fortov, Tech. Phys. Lett. **35**, 1144 (2009).
[29]S. F. Savin, L. G. D'yachkov, M. I. Myasnikov, O. F. Petrov, and V. E. Fortov, Phys. Scr. **85**, 035403 (2012).
[30]V. E. Fortov, A. V. Ivlev, S. A. Khrapak, A. G. Khrapak, and G. E. Morfill, Phys. Rep. **421**, 1 (2005).
[31]M. V. Berry and A. K. Geim, Eur. J. Phys. **18**, 307 (1997).
[32]A. Geim, Phys. Today **51**(9), 36 (1998).
[33]I. E. Tamm, *Fundamentals of Theory of Electricity* (Mir, Moscow, 1979).
[34]S. F. Savin, L. G. D'yachkov, M. I. Myasnikov, O. F. Petrov, M. M. Vasiliev, V. E. Fortov, A. Yu. Kaleri, A. I. Borisenko, and G. E. Morfill, JETP Lett. **94**, 508 (2011).
[35]O. F. Petrov, M. I. Myasnikov, L. G. D'yachkov, M. M. Vasiliev, V. E. Fortov, S. F. Savin, A. Yu. Kaleri, A. I. Borisenko, and G. E. Morfill, Phys. Rev. E **86**, 036404 (2012).
[36]R. Casdorff and R. Blatt, Appl. Phys. B **45**, 175 (1988).
[37]T. Yamanouchi, M. Shindo, O. Ishihara, and T. Kamimura, Thin Solid Films **506**, 642 (2006).